Characterization of Thin Polymer Films on the Nanometer Scale with Confocal Raman AFM

U. Schmidt,[1] *S. Hild,*[2] *W. Ibach,*[1] *O. Hollricher*[1]

Summary: The combination of an atomic force microscope (AFM) with a Confocal Raman Microscope (CRM) has been used to study the composition of various thin films of polymer blends. The high spatial resolution of the AFM enables the morphological characterization of the polymer blends on the nanometer scale. Furthermore, when operating the AFM in Digital Pulsed Force Mode (DPFM), topographic information and local stiffness can be simultaneously recorded. This allows the material-sensitive characterization of heterogeneous materials. Thin films where PMMA (at room temperature a glassy polymer) is blended with two different styrene-butadiene rubbers are investigated. The presence of PMMA in both phase-separated thin films allows the comparison of the mechanical properties of the two different rubber phases using DPFM-AFM. When PMMA is blended with PET due to their similar mechanical properties (both are in the glassy state at room temperature) the assignment of the two phases to the corresponding polymers by AFM is rather difficult. Here, Raman spectroscopy provides additional information on the chemical composition of materials. In combination with a confocal microscope, the spatial distribution of the various phases can be determined with a resolution down to 200 nm. Therefore, the topographically different structures observed in AFM images can be associated to the chemical composition by using the Confocal Raman Microscope (CRM).

Keywords: AFM; polymer blends; Raman spectral imaging

Introduction

The characterization of heterogeneous systems on the microscopic scale continues to grow in importance and to impact key applications in the fields of materials science, nanotechnology and catalysis. The development of advanced polymeric materials for applications such as these requires detailed information about the physical and chemical properties of these materials on the nanometer scale. However, some details about the phase-separation process in polymers are difficult to study with conventional characterization techniques due to the inability of these methods to chemically differentiate materials with good spatial resolution and without damage, staining or preferential solvent washing.

One technique that has been used successfully in the characterization of heterogeneity in polymers is Atomic Force Microscopy (AFM).[1–4] AFM can provide spatial information along and perpendicular to the surface of a polymer film with resolution on the order of 1 nm. The most commonly used AFM imaging mode for polymers is the intermittent contact mode also known as AC Mode or Tapping Mode.[5] In these imaging modes the cantilever is oscillated at its resonance frequency with a free amplitude A_0. While the cantilever is approaching the surface, the oscillating amplitude is reduced to a value A, which depends on the distance to the surface. The ratio $r = A/A_0$ defines the

[1] WITec GmbH, Hörvelsingerweg 6, 89081 Ulm, Germany www.witec.de
[2] Department of Experimental Physics, Central Facilities of Electron microscopy, University of Ulm, Albert-Einstein-Allee 11, 89069 Ulm, Germany

damping of the amplitude while the tip is in contact with the surface and is proportional to the applied force. By keeping the damping of the amplitude constant, the surface topography can be mapped. A phase image can be recorded simultaneously with the surface topography. In this image, the phase shift between the free oscillation in air and the oscillation while the tip is in contact with the surface is recorded.[6] Since the phase shift depends as much on the viscoelastic properties of the sample as on the adhesive potential between the sample and the tip, the phase image outlines domains of varying material contrast without describing the nature of the material properties.[7–11] Nevertheless, phase images are often used to characterize polymers at high resolution.[12,13]

If the AFM is operated in Pulsed Force Mode, information about the local mechanical properties of various regions on the sample surface can be obtained more quantitatively.[14] In this imaging mode, a sinusoidal modulation is imposed on the cantilever typically with a frequency of 1 kHz, which is far below the resonance frequency of the cantilever. Thus, the applied force can be controlled using the beam deflection technique while the cantilever is approached to and retracted from the sample. The pulsed force curve shows the variation of the force signal as a function of time. Therefore it contains all information about the tip-sample interaction. The resulting pulsed force curve obtained during the whole cycle is recorded at every image point.[15] In this mode quantified material properties can be mapped together with the topography of the films.[16]

Although these imaging modes have been successfully applied in the characterization of polymer blends, the differentiation of materials is only possible by comparing their material properties, such as local stiffness. This is mainly due to the lack of information about the exact contact area between tip and sample. If a composite material consists of compounds with similar mechanical properties, a clear assignment of the phases to the corresponding materials by AFM is quite challenging. To discriminate between materials with similar mechanical properties additional spectroscopic information is useful. On the macroscopic scale, Raman spectroscopy has become widely used for the characterization of chemical and structural features of polymeric materials.[17] The tremendous importance of the Raman effect lies in the fact that the difference in energy between the elastically scattered photons and the Raman shifted photons is caused by the excitation or annihilation of a specific molecular vibration. This energy shift is characteristic for the type and coordination of the molecules involved in the scattering process. Raman spectra provide qualitative and quantitative information about various polymer features[18–20] such as:

- chemical nature: structural units, type and degree of branching, end groups, additives
- conformational order: physical arrangement of the polymer chain
- state of order: crystalline, mesomorphous and amorphous phases
- orientation: type and degree of polymer chain and side group alignment in anisotropic materials.

However, in most spectroscopy setups the spatial resolution is very poor because the exciting laser spot diameter is on the order of 100 μm.

Optical microscopy, on the other hand, is capable of providing spatial resolution down to 200 nm using visible light excitation. In a confocal microscope, the light from the sample is detected through a pinhole in the back focal plane of the microscope, giving rise to depth resolution and a strongly reduced background signal.[21] By combining a high throughput confocal microscope with an extremely sensitive Raman spectroscopy system, it is possible to obtain Raman spectra from extremely small sample volumes down to 0.02 μm^3. To collect high resolution Raman images, the sample is scanned point by

point and line by line through the excitation focus.[22] Thus, the Confocal Raman Microscope (CRM) combines the chemical sensitivity of Raman spectroscopy and the high resolution of confocal microscopy, providing an ideal tool for the characterization of materials in the sub-micrometer range. To achieve the highest resolution, the CRM is extended with AFM capabilities. By simply rotating the microscope turret, the user can link the chemical information obtained by confocal Raman spectroscopy with the ultra-high spatial and topographical information acquired by AFM.

The aim of this paper is to demonstrate the capabilities of the Confocal Raman-AFM in terms of the characterization of thin heterogeneous polymer films. For this purpose three blends composed of immiscible polymers, which are at room temperature in either the rubbery or glassy state are investigated.

Experimental Section

Materials and Sample Preparation

Poly(ethylene terephthalate) (PET) films and styrene butadiene (SB) copolymers with a styrene content of 30% were acquired from Sigma Aldrich. For the triblock copolymer (SBS), a molar mass M_W of 74 kg/mol, and for the statistical copolymer (SBR) a molar mass M_W of 380 kg/mol were measured using GPC (calibrated for poylstyrene). Poly(methyl methacrylate) (PMMA) with a M_W of 100 kg/mol was purchased from Polymer Standards. From these materials, polymer solutions are prepared by dissolving 10 mg of the polymer in 1 ml solvent. The styrene butadienes are soluble in toluene, but PET is only soluble in hexafluoroisopropanol (HFIP). Therefore, PMMA is dissolved in both toluene and HFIP. Blends are prepared by mixing either 2 ml of the PMMA toluene solution and 1 ml of the SBS or SBR solutions or 2 ml of the PMMA HFIP solution and 1 ml of PET solution.

Thin films with a thickness of less then 100 nm were obtained by spin coating pure polymer solutions as well as blended ones on cleaned glass substrates (cover slides) using spinning velocities of 2000 rpm. Characterization by AFM and CRM are performed at room temperature immediately after spin coating.

Atomic Force Microscopy

The Confocal Raman-AFM from WITec (www.witec.de) was used for AFM imaging in ambient conditions ($24 \pm 2\,^{\circ}C$). For high resolution imaging the AFM was operated in AC-Mode with a damping of $r = 50\%$ where topography and phase images are recorded simultaneously. Additionally, the samples were imaged in Digital Pulsed Force Mode to designate areas of different mechanical properties. For all experiments ''Arrow Force Modulation'' cantilevers purchased from Nanoworld were used, which allow switching from one imaging mode to the other on the same sample area. The nominal spring constant of this cantilever is 2.8 N/m and the resonance frequency ranges between 70–80 kHz. The DPFM was operated at a modulation frequency of 1 kHz, with cantilever oscillation amplitudes up to 300 nm.

Confocal Raman Microscopy

The Confocal Raman-AFM was used to collect single Raman spectra from the pure polymer and Raman spectral images from the films of polymer blends. A Nikon 100x ($NA = 0.90$) objective was employed for all measurements. For excitation, a NdYag laser (wavelength of 532 nm) was used. The Raman spectra of the pure polymers were recorded with an integration time of 100 ms. Polymer blends were analyzed in Raman spectral imaging mode. In this mode, high resolution Raman images are obtained by collecting a complete Raman spectrum at every image pixel (up to $512 \times 512 = 262144$ spectra) with typical integration times below 100 ms/pixel. The analysis of spectral features (sum, peak position, peak width etc.) generates the Raman images.

Results and Discussion

AFM topography images reveal that both glassy polymers, PMMA (Figure 1a) as well as PET (Figure 1b), do not cover the glass slide completely, but form a porous structure. In the PMMA film, the holes are about 100 nm deep with diameters ranging from 100–500 nm which lead to a net-like morphology of the film. In the PET film, the diameter of the holes is below 200 nm and their depth is about 30 nm.

These structural variations give evidence that the solubility of the polymers in HFIP might be different. In contrast to this, the SB films appear smooth without any corrugations in topography. However, high-resolution AC Mode phase images reveal a phase-separated structure of the rubbery polymers. In the phase images, brighter areas can be assigned to the harder (glassy) polystyrene domains whereas the rubbery butadiene domains appear dark. In SBR, where small polystyrene blocks are statistically distributed, this phase forms spheres with a diameter of about 25 nm (Figure 1c). The long polystyrene blocks, present in the triblock copolymer SBS, aggregate to a wormlike structure as shown in Figure 1d. These variations in the polymer nano-structure are in good agreement with previously reported data.[23,24]

The two types of styrene-butadiene (SB) were blended with PMMA into PMMA-SBS and PMMA-SBR. In Figure 2, DPFM-AFM images of these heterogeneous blends are presented. On a scan area of 7×7 μm^2, the PMMA-SBR blend (Figure 2a) reveals elevated circular islands with diameters in the range from 500 nm to 2 μm in the topography image. The PMMA-SBS blend forms a netlike elevated structure (Figure 2b). In between the

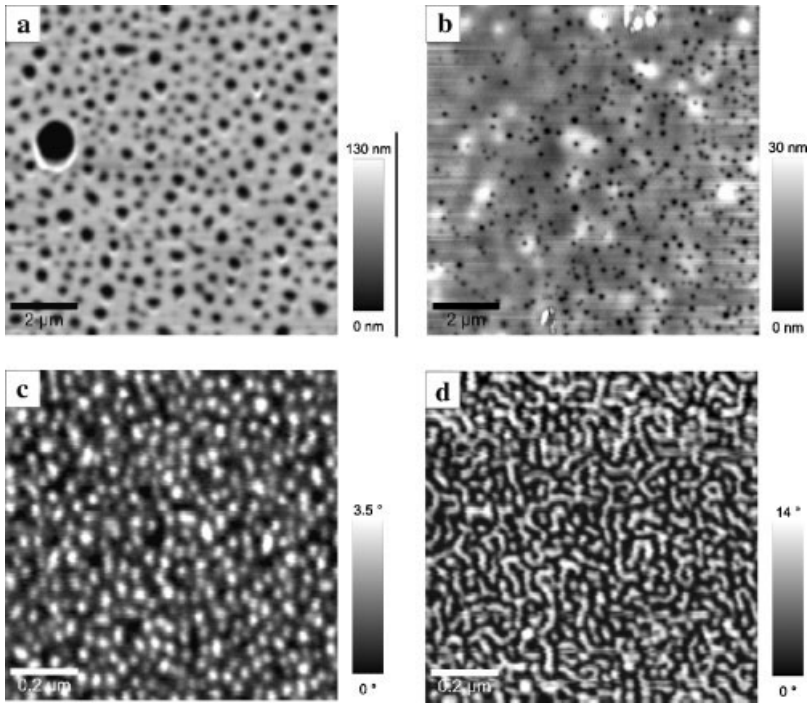

Figure 1.
AFM images of pure polymer films spin coated on glass substrates: a) PMMA topography image scan size: 10×10 μm^2, b) PET topography image scan size: 10×10 μm^2, c) SBR phase image scan size: 1×1 μm^2 and d) SBS phase image scan size: 1×1 μm^2.

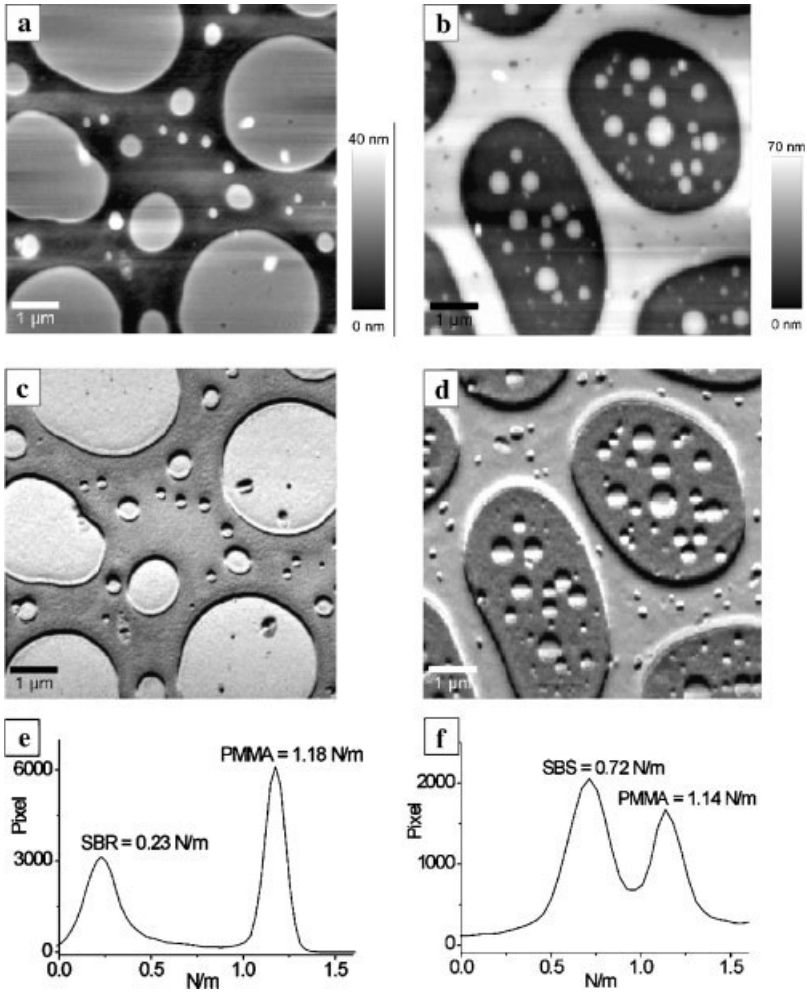

Figure 2.
DPFM measurements on polymer blend PMMA-SB: topography of blend a) PMMA-SBR and b) PMMA-SBS; simultaneously recorded stiffness maps c) PMMA-SBR and d) PMMA-SBS; histogram of stiffness distribution e) PMMA-SBR and f) PMMA-SBS. Scan size of all four images: $7 \times 7\ \mu m^2$.

elevated features, a lower polymeric phase can be seen in both blends. Since SB and PMMA are immiscible, the different topographic structures can be associated to the various polymer phases. This gives strong evidence for the formation of a phase-separated morphology of the films due to dewetting.

Simultaneously recorded stiffness maps (Figures 2c and d) allow the assignment of topographical features to different polymer phases. The elevated topographic features also show higher stiffness (bright colors in stiffness map) compared to the lower topographic regions, which have lower stiffness. Based on macroscopic mechanical properties, the stiffer phase corresponds to PMMA, which is in the glassy state at room temperature.[25] The softer phase can be assigned to SB, which has a glass transition temperature far below room temperature, thus leaving it in a rubbery state.[26]

To quantify the stiffness maps, the measured voltages of the stiffness output ($V_{stiffness}$) of the DPFM electronics are converted into the physical unit of the local

stiffness (N/m) using the relation:[27]

$$\text{Stiffness} = k\,S\,V_{\text{stiffness}}/[M(1-\cos(2\pi f \Delta t) - S\,V_{\text{stiffness}}] \quad (1)$$

with k being the spring constant of the cantilever, S the sensitivity of the laser detection system, M the modulation amplitude, f the modulation frequency, and Δt the repulsive tip penetration time.

After unit conversion of the stiffness maps, the histograms shown in Figure 2 (e and f) are obtained. Both histograms show two peaks. The one, which appears for both blends at 1.15 ± 0.1 N/m, can be correlated to the stiffer PMMA. The other at lower stiffness values can be assigned to the SB phase. For SBS an average stiffness of 0.7 ± 0.1 N/m and for SBR an average stiffness of 0.2 ± 0.1 N/m are evaluated. Since the average stiffness of PMMA in both blends is the same, it can be used as an internal reference for the comparison of the stiffness properties of SBS and SBR. In comparing the stiffness data obtained for the PMMA-SB films, values indicate that SBS is stiffer than SBR by a factor of 3.5.

High-resolution AC Mode AFM images (Figure 3) confirm the structural differences found in the DPFM images. In both films, the topography reveals 20–30 nm high features showing bright islands without texture in the simultaneously recorded phase images. The islands are surrounded by a phase showing different fine structures characteristic of the various SB's. In Figure 3b the fine structure of SBR is visible, whereas in Figure 4b the wormlike structures observed in the pure SBS film can be visualized (compare Figures 1 c and d). These images allow the assignment of differences in local stiffness to different morphologies of the styrene-butadiene copolymers. The copolymer showing larger extended (worm-like) domains of the polystyrene is seen on the microscopic scale to be stiffer than the copolymer with small randomly distributed styrene spheres in the butadiene phase. This is in agreement with the macroscopic properties.

In Figure 4 the topographical structure of the PMMA-PET blend is shown together with the height distribution histogram. The histogram clearly shows three topographic levels: a ground level with height below 50 nm associated with the dark areas, a 100 nm high porous film, and a 200 nm high net-like structure. This three level structure indicates a superposition of two network-like structures. Since both PMMA and PET are rather stiff materials with similar elasticity modulus, a separation of the two polymer phases based on local stiffness measurements as shown before is ambiguous. To determine the chemical composition of the phase-separated films, the selective dissolution of one of the polymer phases has been employed in previous studies.[28,29] After applying this method, however the films are destroyed.

A non-destructive characterization with respect to the chemical composition of polymer blends is possible using spectroscopy methods such as Raman spectroscopy. The ability to employ Raman spectroscopy for the analysis of thin films is shown in Figure 5. The single Raman spectra of the pure polymer films spin coated on glass substrates together with the Raman spectrum of pure glass are shown. The Raman spectrum of glass shows broad bands at wavenumbers below 1200 cm^{-1} and is featureless at higher wave numbers. These broad bands below 1200 cm^{-1} are visible in all single Raman spectra collected on the polymer films, indicating that the film thickness is below the z-resolution of the optical confocal microscope, which is about 500 nm. Nevertheless, at wave numbers above 1200 cm^{-1}, the characteristic polymer Raman bands are clearly be visible.

All polymer samples show characteristic band structures in the range 2800–3100 cm^{-1}, which is associated with C–H stretching and peaks at 1460 cm^{-1}, which is characteristic for C–H bending.[30] In addition, each polymer sample reveals additional characteristic peaks associated with molecular vibrations observed for the

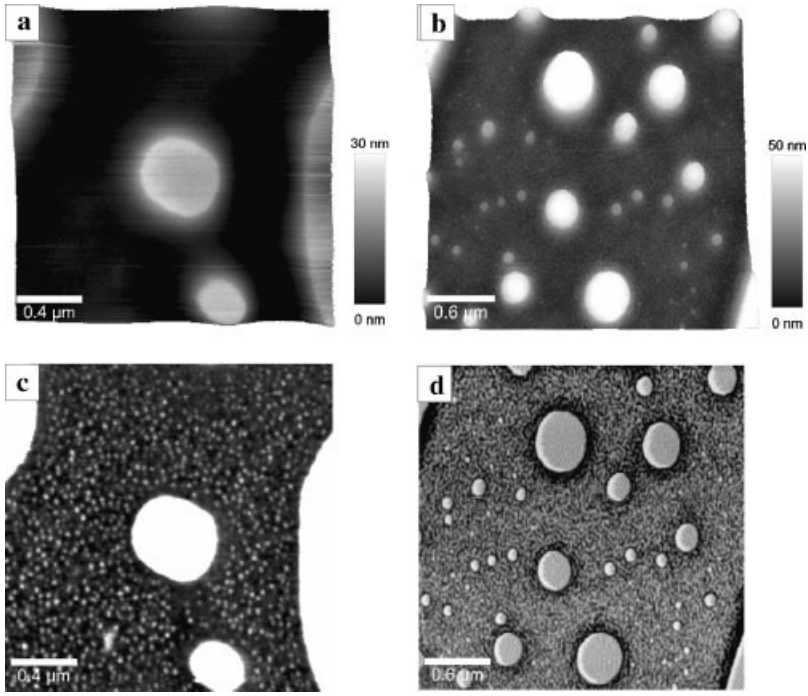

Figure 3.
High resolution AC Mode AFM image of the polymer blend PMMA-SB. Topography of a) SBR (image size: 2 × 2 μm^2) and b) SBS (image size: 3 × 3 μm^2) and simultaneously recorded phase images of c) SBR and d) SBS.

different polymers as summarized in Table 1.[26] In PMMA, a band appears at 1730 cm^{-1} correlating to C=O stretching. In the PET Raman spectrum, additional Raman bands associated with benzene ring vibrations at 1192 cm^{-1} and 1615 cm^{-1} are visible. The Raman spectra collected from the SB films show Raman bands characteristic for C=C stretching at 1635–1650 cm^{-1}. For both polymers (SBS and SBR), Raman bands can be found at the same wave number indicating the same chemical composition. However, the variations in the intensity of peaks, e.g. at 1635–1650 cm^{-1}, reflects the

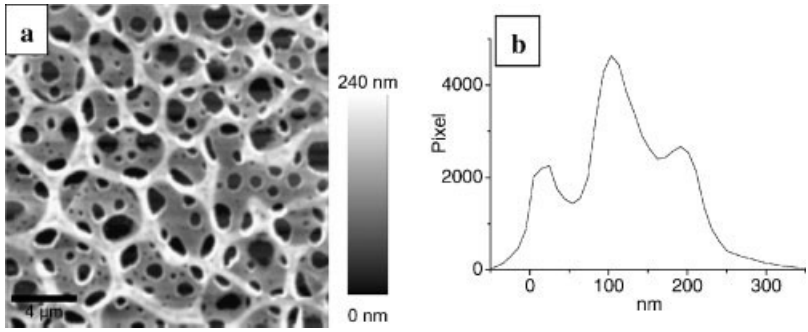

Figure 4.
a) AFM topography image of the thin film of polymer blend PMMA – PET (image size: 20 × 20 μm^2) and b) height distribution histogram.

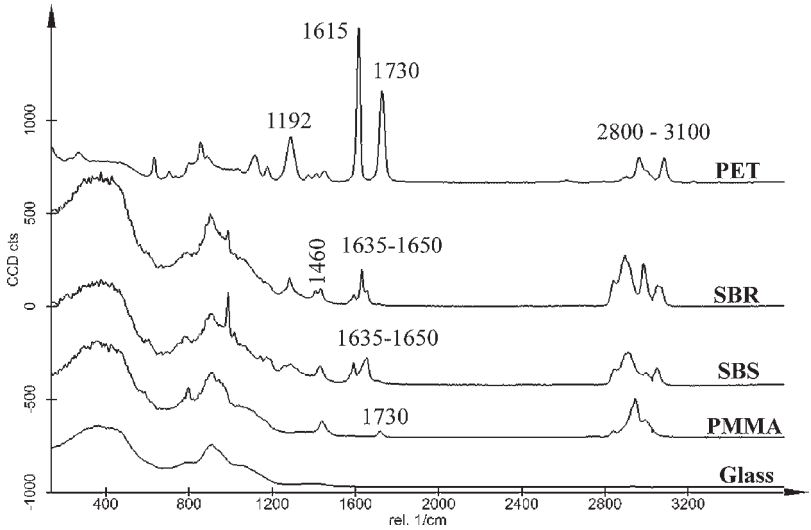

Figure 5.
Single Raman spectra collected on the pure films of polymer spin coated on glass substrates.

structural differences of the two films as observed in the AFM images.

The variations in the Raman spectra make it possible to distinguish the various polymers from each other when they are blended. Therefore, the thin films of polymer blend were scanned in Raman spectral imaging mode.

In this mode, a complete Raman spectrum is recorded at every image pixel ($200 \times 200 = 40000$ spectra) with integration times below 100 ms. To assign the different polymers in the film, not only were individual features (such as peak position, peak width, etc) of the Raman spectra employed, but the complete spectra of the materials by using basis spectra analysis. In this procedure each measured spectrum of the 2-dimensional data array is fitted by a linear combination of basis spectra S_k using least squares method. Each material has a unique Raman spectrum S_k, called a basis spectrum. A sample which consists of N different materials shows a linear superposition of all its basis spectra

$$S = \Sigma a_k S_k \qquad (2)$$

with $k = 1$ to N.

If the basis spectra S_k are known as in this case (see Figure 5), it is possible to estimate the weight factor a_k by a least squares fit. The weighting factor is proportional to the quantity of the material and is stored in the corresponding Raman image.

Figure 6a shows the background corrected spectra of PMMA, PET and glass, revealing the complete Raman spectrum of the polymers. These spectra were used in the basis analysis of the Raman spectral image recorded from the thin film of the

Table 1.
Characteristic Raman bands from measured spectra of pure polymer films.

Raman band (cm^{-1})	Molecular vibration	Observed in Raman spectrum of:
1192	Ring mode	PET
1460	C–H bending	**PMMA**, PET
1635–1650	C=C stretching	SBS, SBR
1730	C=O stretching	**PMMA**, PET
2800–3100	C–H stretching	**PMMA**, PET, SBS, SBR

polymer blend PMMA-PET. In Figure 6b the 2-dimensional distribution of the weight factor a_1 of the PET spectrum is shown, illustrating the presence of PET on specific areas on the surface. Figure 6c shows the distribution of PMMA evaluated by basis analysis. These two images show that the two polymer phases are completely separated because no overlap of PMMA and PET can be seen. Combining the images of Figures 6b and 6c results in the distribution of the PET and PMMA phases within the blend (Figure 6d). This image confirms the assumption that the two topographic layers are superposed (compare with Figure 4).

The various topographic layers observed with the AFM can now be assigned to the chemical species in the following way: the high netlike topographic structure corresponds to PET, the lower layer consists of PMMA. The holes within this layer are areas where the polymer does not cover the glass slide.

The phase separation within the thin films of the polymer blend PMMA-SB has also been proven by CRM measurements in spectral imaging mode. Figure 7a show the basis spectra of SBR, SBS and PMMA used as basis spectra for data analysis of the image spectra. An overlay of the fitted data is shown in Figures 7b and c, where bright color represents the PMMA phase and dark color the distribution of the SBR respectively the SBS phase. The Raman spectral images of the blends of PMMA–SB show a structure similar to the topographic DPFM images (compare with Figure 2 and b). Elevated domains in the topographic DPFM images were associated with the stiffer PMMA and are in good agreement

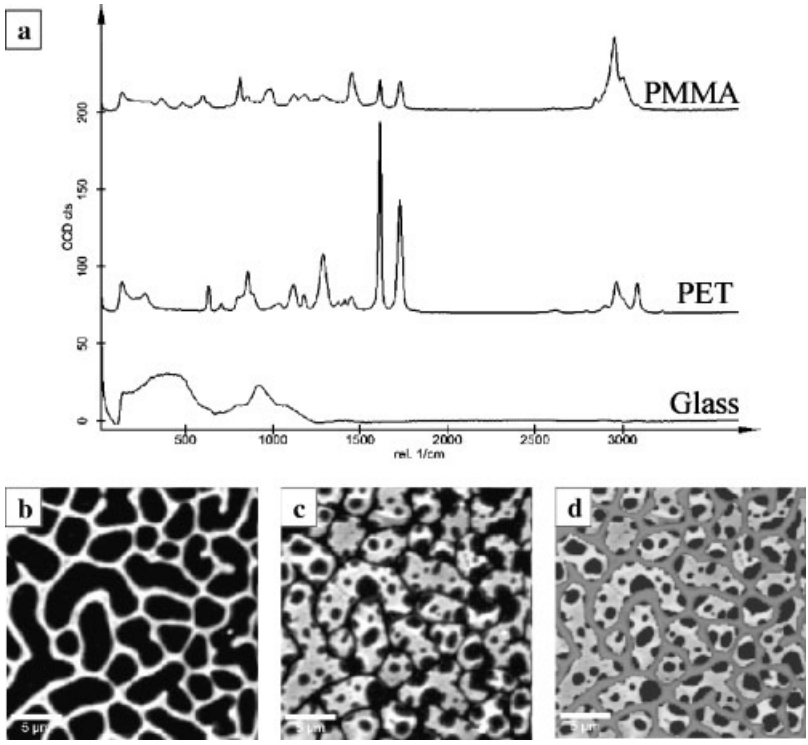

Figure 6.
a) Basic spectra of PMMA, PET and glass used for basis analysis of the Raman spectral image data obtained on the polymer blend PMMA-PET, b) distribution of PET and c) PMMA calculated by basis analysis, and d) overlay of PMMA and PET Raman images showing the distribution of the two polymer phases over the surface. (image size: $25 \times 25\ \mu m^2$).

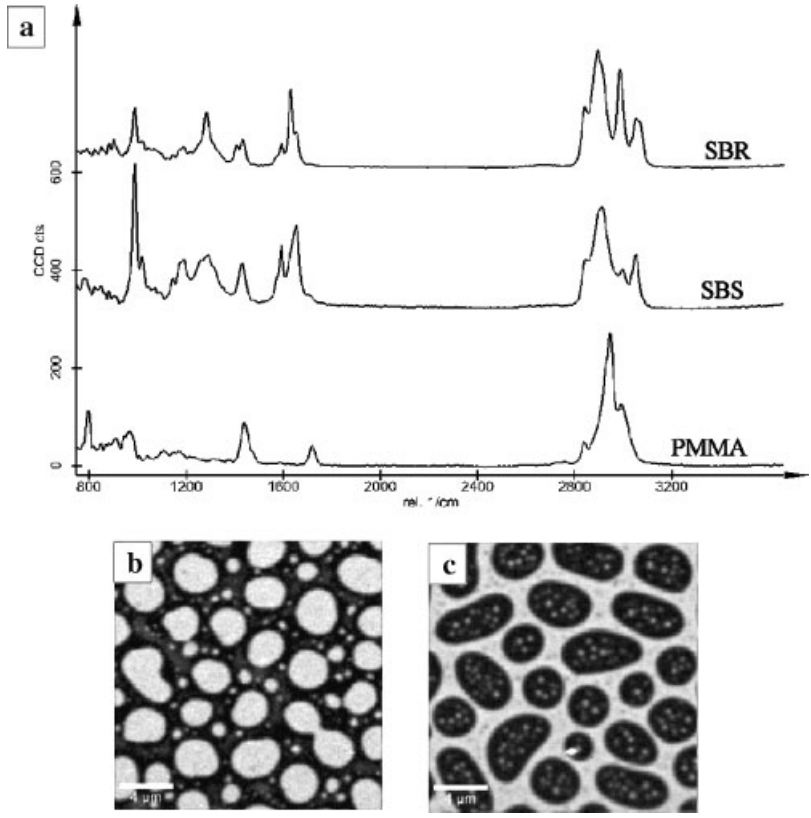

Figure 7.
a) Basic spectra of PMMA and SB and b) phase separated spectral images with $20 \times 20\ \mu m^2$ scan area of PMMA-SBR and c) PMMA-SBS, with PMMA as bright areas. As the Raman spectral images show, the distributions of PMMA and SB are complementary, proving that both polymer phases are formed on the glass substrate.

with the distribution of the PMMA phase in the Raman spectral image.

Conclusions

The combination of a Confocal Raman Microscope with an AFM is used for the characterization of polymer blends. AFM images reveal the topographic structure of polymer films with resolution down to a few nanometers. The high-resolution AFM phase images allow the identification of two styrene-butadiene copolymers (SBR and SBS) with different chain-microstructures. Well-separated domains are formed when these polymers are blended with PMMA and spin coated on a glass substrate. The comparison of their mechanical properties estimated from DPFM local stiffness maps shows that SBS is 3.5 times stiffer than SBR. This is in good agreement with the observed fine structure on the nanometer scale, where within the triblock copolymer, the harder styrene blocks form more extended domains.

Raman spectroscopy allows the identification of chemically unique materials. In combination with a confocal microscope, the distribution of various polymer phases within the films can be determined. Due to the confocal principle, not only can the surface be investigated, but information to a certain depth within the film can be also obtained. The analyzed very thin polymer films ($z < 200$ nm) show clear Raman spectra of the corresponding polymers, indicating that a small sample volume

(below 0.02 μm^3) is enough to identify the chemical composition of the film. The analysis of the Raman spectral images, obtained from the blended films show that there is no overlap of basis spectra at any image point. This indicates that the studied polymers do not cover each other but have formed an interface with the glass substrate while dewetting. In the polymer blend consisting of PMMA and PET, which are both in the glassy state at room temperature, a superposition of two net-like structures is observed with AFM. The assignment of the two phases is possible with Raman spectral imaging, showing that the elevated net-like structure observed with the AFM corresponds to PET, whereas the porous film is PMMA. These two structures do not overlap, they are completely separated and form an interface with the glass substrate.

The combination of AFM and CRM in a single instrument enables the nondestructive characterization of heterogeneous materials. The surface topography can be imaged at the highest resolution and various materials contributing to the surface composition can be chemically identified.

Acknowledgements: The authors like to thank Damon Strom for careful reading and correcting the manuscript.

[1] W. Stocker, J. Beckmann, R. Stadler, J. Rabe, *Macromolecules* **1999**, *29*, 7502.
[2] N. Koneripalli, R. Levicky, F. S. Bates, J. Ankner, H. Kaiser, S. K. Satija, *Langmuir* **1996**, *12*, 668.
[3] T. J. Morkved, H. M. Jaeger, *Europhys. Lett.* **1997**, *40*, 643.
[4] R. S. McLean, B. B. Sauer, *J. Polym. Sci., Part B* **1999**, *37*, 85.
[5] Q. Zhong, D. Inniss, K. Kjoller, V. Ellings, *Surf. Sci.* **1993**, *290*, L688.
[6] S. N. Magonov, V. Elings, M.-H. Whangbo, *Surf. Sci.* **1997**, *372*, L385.
[7] J. Tamayo, R. Garcia, *Appl. Phys. Lett.* **1997**, *71*, 2394.
[8] J. Tamayo, R. Garcia, *Appl. Phys. Lett.* **1998**, *73*, 2926.
[9] R. Garcia, J. Tamayo, A. Paolo, *Surf. Interface Anal.* **1999**, *27*, 312.
[10] J. P. Cleveland, B. Anczykowski, A. E. Schmid, V. B. Elings, *Appl. Phys. Lett.* **1998**, *72*, 2613.
[11] W. W. Scott, B. Bhushan, *Ultramicroscopy* **2003**, *97*, 151.
[12] G. Bar, Y. Thomann, R. Brandsch, H.-J. Cantow, M.-H. Whangbo, *Langmuir* **1997**, *13*, 3807.
[13] S. Hild, O. Marti, F. Hollmann, B. Rieger, *Europ. Polym. Journ* **2004**, *40*, 905.
[14] A. Rosa, E. Weilandt, S. Hild, O. Marti, *Meas. Sci. Techn.* **1997**, *8*, 1.
[15] A. Gigler and O. Marti, "Pulsed Force Mode SFM, in SPMs beyond imaging", edited by P. Samori (2005).
[16] H.-U. Krotil, T. Stifter, H. Waschipky, K. Weishaupt, S. Hild, and O. Marti, *Surface and Interface Analysis* **1999**, *27*, 336.
[17] H. W. Siesler and K. Holland-Moritz, "*Infrared and Raman Spectroscopy of Polymers*", Marcel Dekker, New York, 1990.
[18] H. Owen, D. E. Battery, M. J. Pelletier, and J. B. Slater, *SPIE Proc.* **1995**, *2406*, 260.
[19] E. D. Lipp and R. L. Grosse, *Appl. Spectrosc.* **1998**, *52*, 42.
[20] J. F. Aust, K. S. Booksh and M. L. Myrick, *Appl. Spectrosc.* **1996**, *50*, 382.
[21] T. Wilson, "*Confocal Microscopy*", Academic Press, London 1990.
[22] O. Hollricher, *OE Magazine*, Nov. **2003**.
[23] M. Konrad, A. Knoll, G. Krausch, R. Magerle, *Macromolecules* **2000**, *33*, 5518.
[24] N. Rhese, A. Knoll, R. Magerle, G. Krausch, *Macromolecules* **2003**, *36*, 3261.
[25] K. C. Berger, G. Meyerhof, in: "*Polymer Handbook*", 3rd ed., J. Brandup, E. H. Immergut, Eds., J. Wiley & Sons, New York 1989, p. V78.
[26] K. C. Berger, G. Meyerhof, in: "*Polymer Handbook*", 3rd ed., J. Brandup, E. H. Immergut, Eds., J. Wiley & Sons, New York **1989**, p. V9.
[27] P. Spizig, Ph.D. Thesis, University of Ulm, 2002.
[28] P. Cyganik, A. Budkowski, J. Raczkowska and Z. Postawa, *Surface Science* **2002**, *507–510*, 700.
[29] S. Walheim, M. Ramstein, U. Steiner, *Langmuir* **1999**, *15*, 4828.
[30] F. J. Boerio, S. K. Bahl, and G. E. McGraw, *J. Polym. Sci., Polym. Phys. Edn.* **1976**, *14*, 1029.

